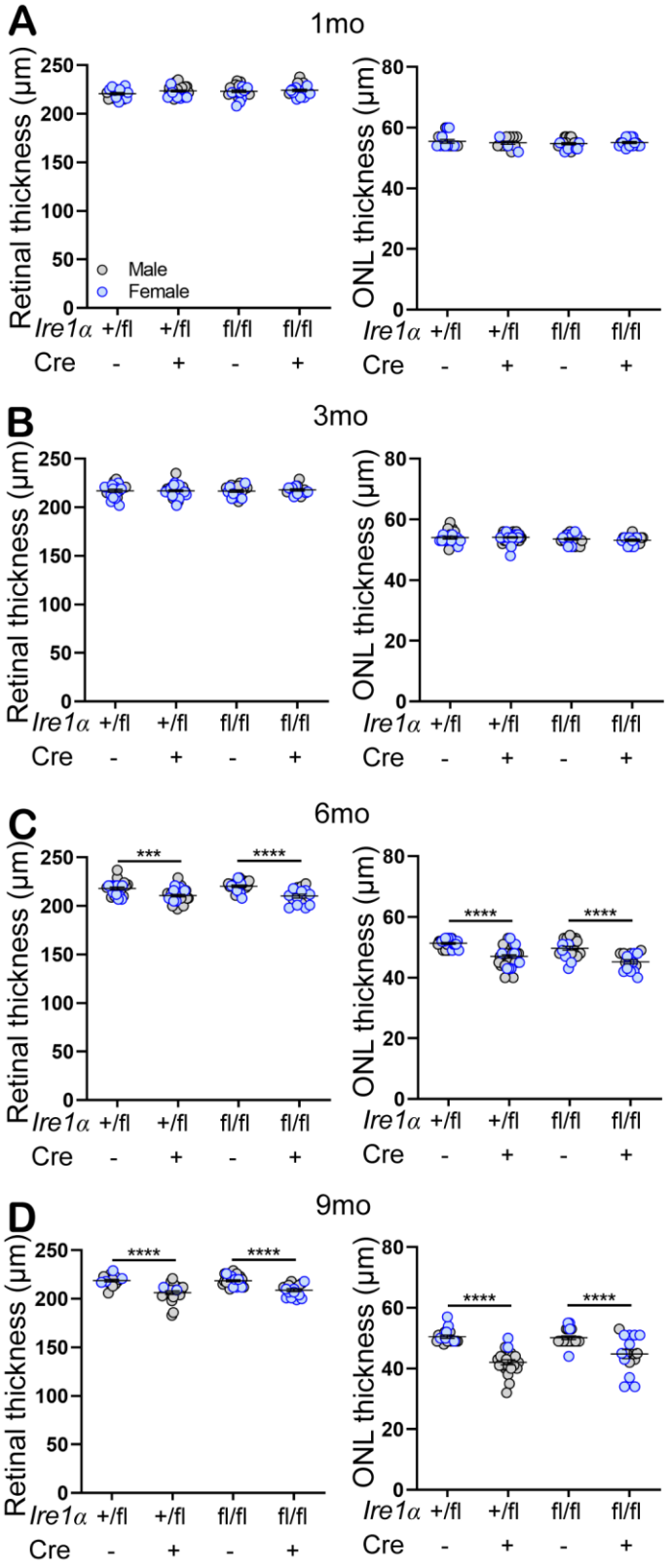
A
1mo
Retinal thickness (μm)
ONL thickness (μm)
Male
Female
Ire1α +/fl +/fl fl/fl fl/fl
Cre - + - +
B
3mo
C
6mo
***
****
D
9mo

Fig. S1: IRE1α deficiency in rod photoreceptors induces age-related retinal degeneration. (**A-D**) OCT measurements showing retinal and ONL thickness of IRE1α deficient retinas at 1, 3, 6 and 9 months old, respectively showing no sex influence at any analyzed time point. Data are presented as mean ± SEM. ***p < 0.001, ****p < 0.0001; two-tailed Student's t-test.

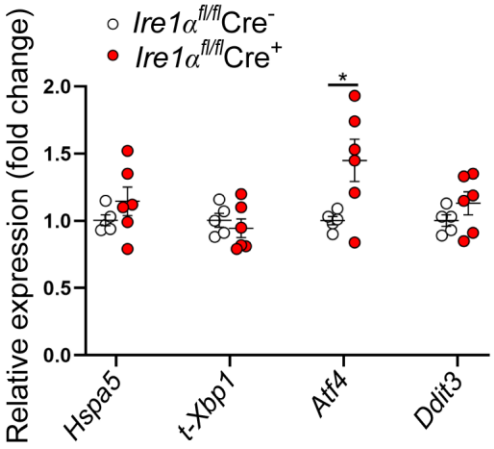

Fig. S2: PERK pathway is increased in IRE1α deficient retinas. qPCR data from 1 month old IRE1α deficient retinas showing an increase in the expression of *Atf4* that is downstream of PERK while *Ddit3*, *Hspa5* and *Xbp1* remain unchanged (n=5-6). Data are presented as mean ± SEM. *p < 0.05; two-tailed Student's t-test.

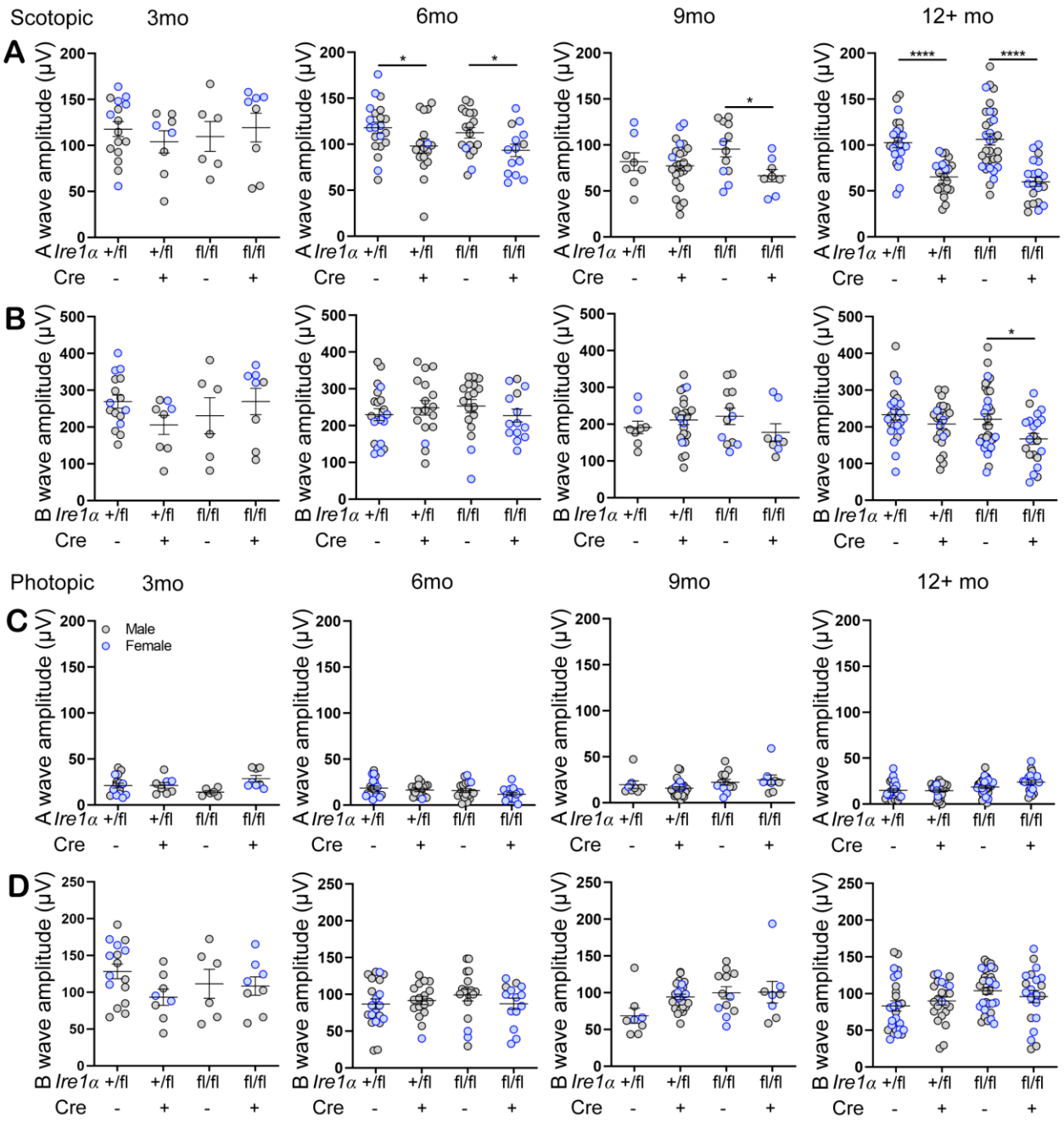

Fig. S3: IRE1α deficiency in rod photoreceptors causes retinal functional deficits. (**A** and **B**) are scotopic and (**C** and **D**) are photopic ERGs recordings at 3, 6 and 9 months old represented by sex and showing a similar distribution between males and females at every recorded time point. Data are presented as mean ± SEM. *p < 0.05, ****p < 0.0001; two-tailed Student's t-test.

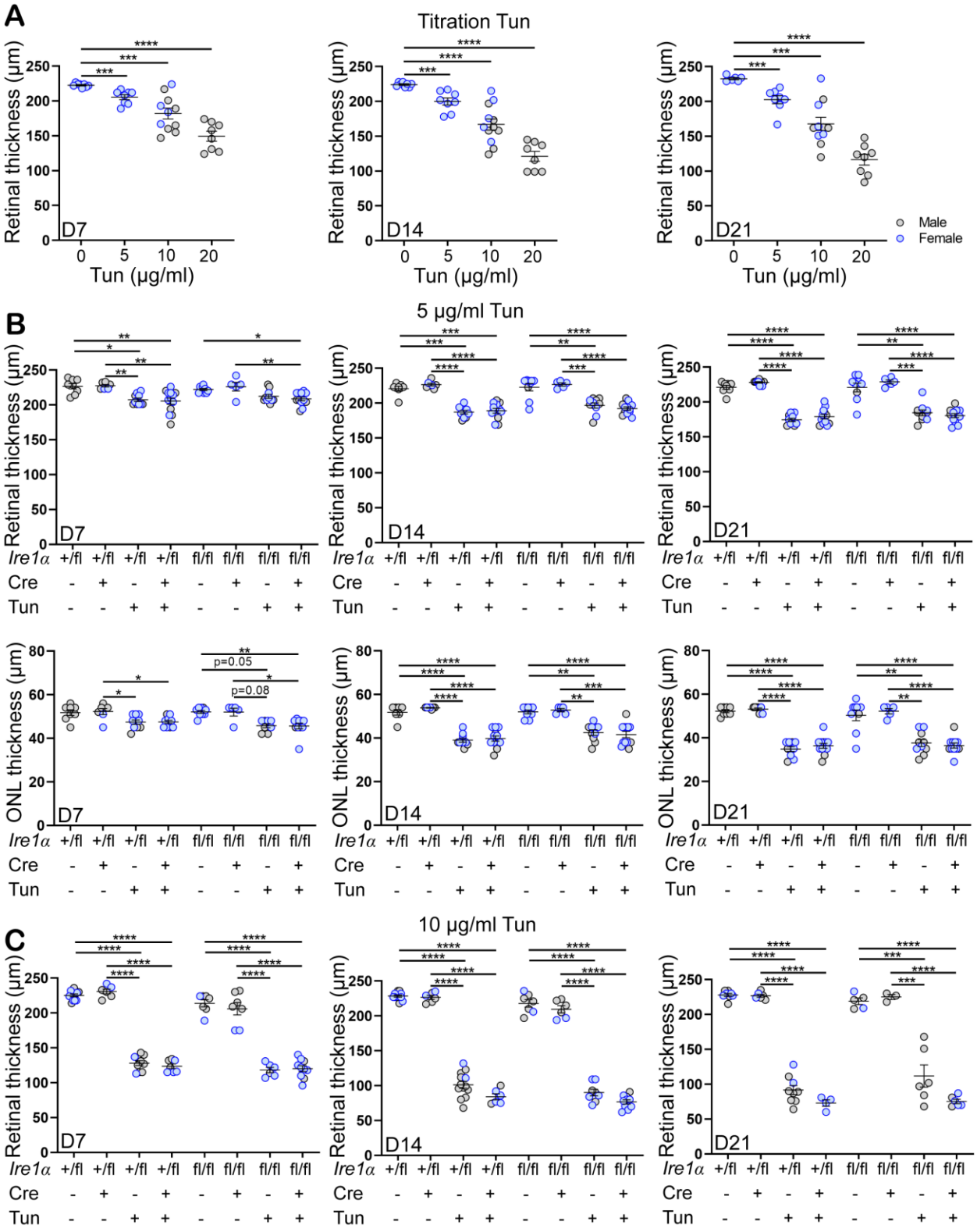

Fig. S4: Sex does not influence retinal thickness in response to chemically induced ER stress. OCT measurements of retinal and ONL thickness following intravitreal injection of tunicamycin. The data indicate that tunicamycin-induced retinal degeneration affects males and

females similarly for both the wild type (**A**) and IRE1α deficient retinas (**B** and **C**). Data are presented as mean ± SEM. *p < 0.05, **p < 0.01, ***p < 0.001, ****p < 0.0001; two-tailed Student's t-test for wild type mice and two-way ANOVA for IRE1α deficient retinas. Tun, tunicamycin.

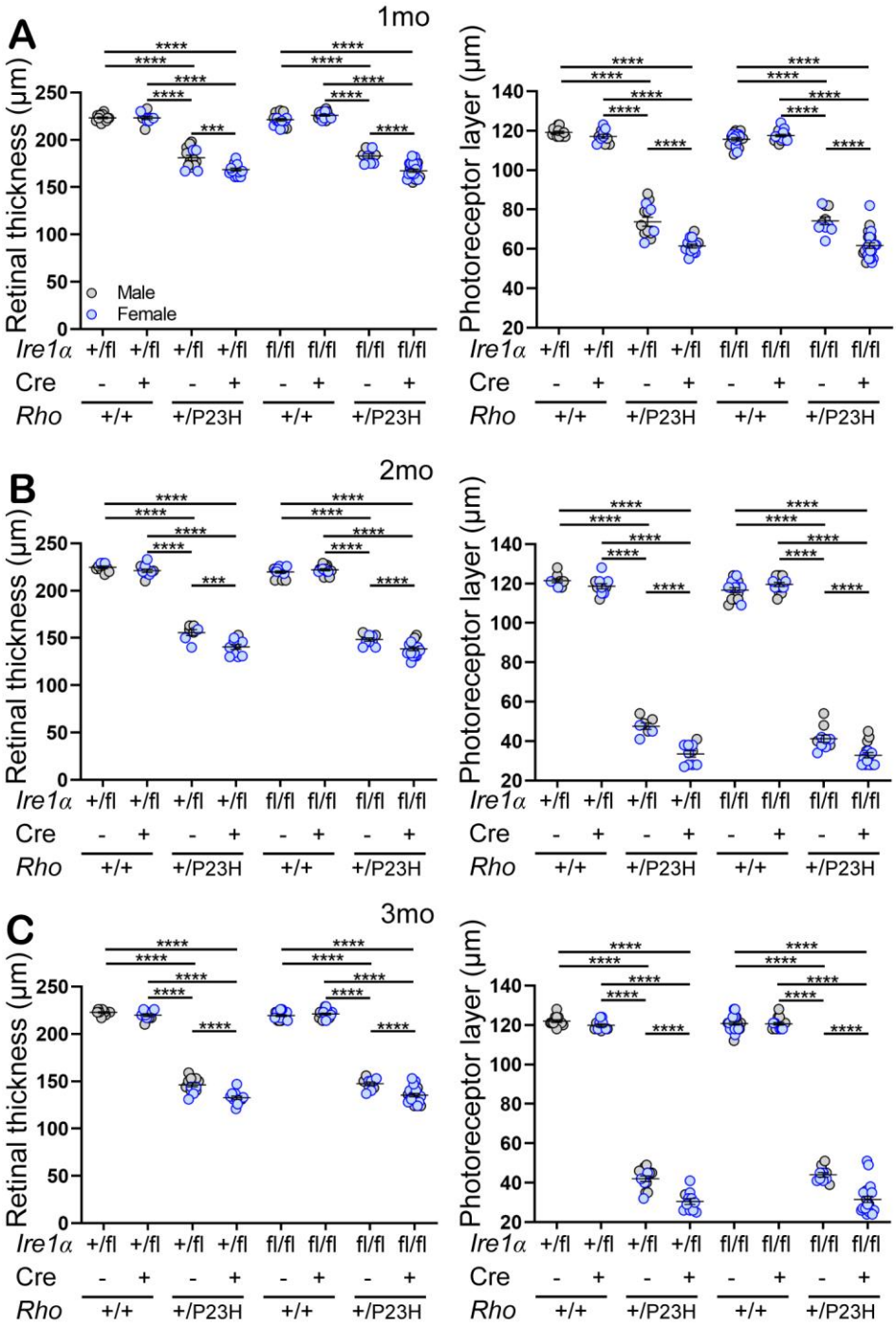

Fig. S5: Inactivation of *Ire1α* in rod photoreceptors affects similarly the males and females in retinal degeneration caused by *Rho*^{P23H} mutation. (**A-C**) OCT data of IRE1α deficient mice in *Rho*$^{+/P23H}$ or *Rho*$^{+/+}$ background at 1, 2, and 3 months old respectively, showing a similar variation of retinal and photoreceptor layer thickness between males and females. Data are presented as mean ± SEM. ***p < 0.001, ****p < 0.0001; two-way ANOVA.

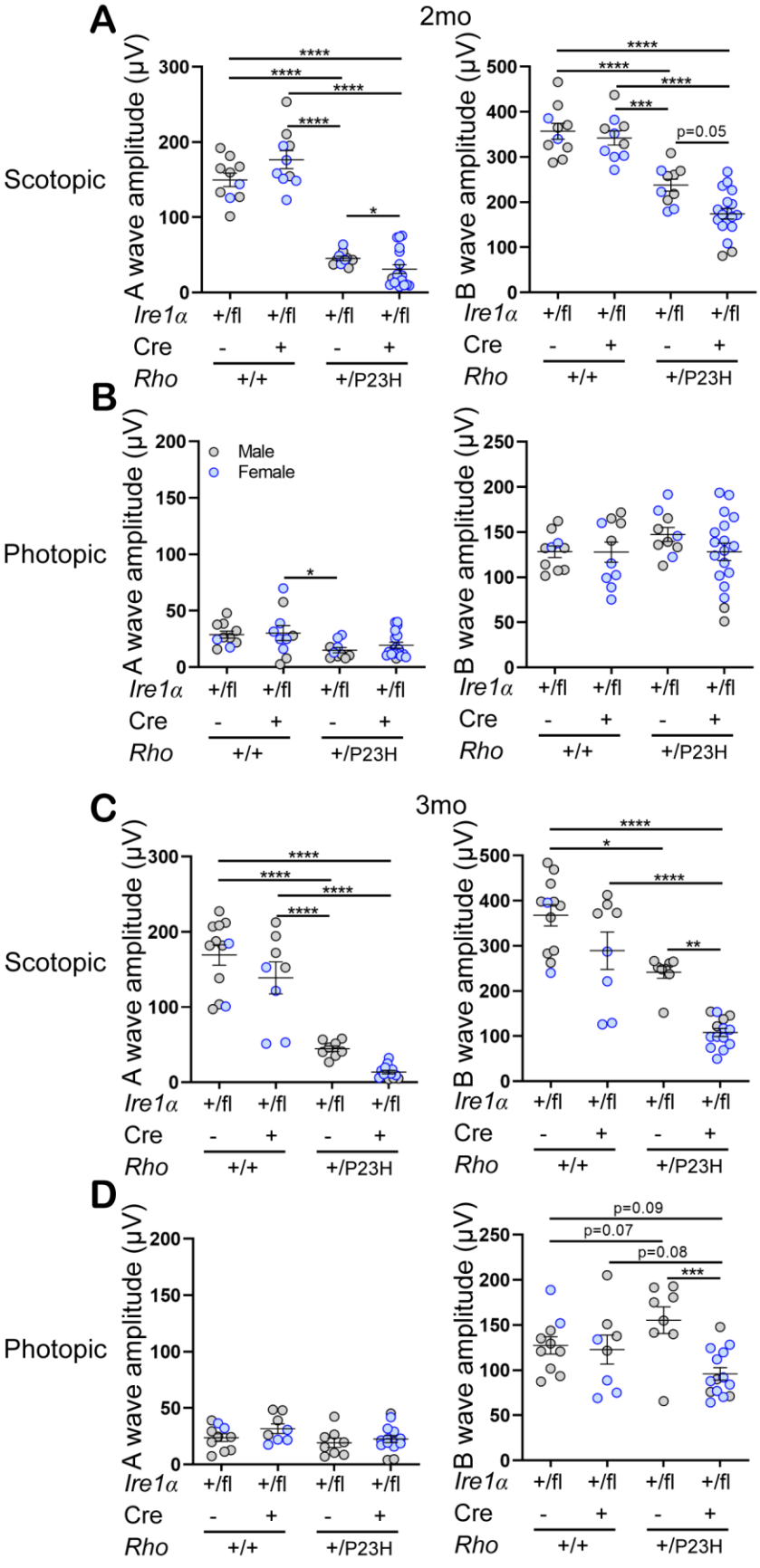
A
2mo
Scotopic
A wave amplitude (μV)
B wave amplitude (μV)
Ire1α +/fl +/fl +/fl +/fl
Cre - + - +
Rho +/+ +/P23H
p=0.05
B
Photopic
Male
Female
C
3mo
Scotopic
D
Photopic
p=0.09
p=0.07
p=0.08

Fig. S6: IRE1α deficiency in rod photoreceptors tends to exacerbate retinal functional deficits caused by *Rho*^{P23H} mutation and affects similarly males and females. (**A** and **C**) are scotopic ERGs recordings at 2, and 3 months respectively, showing decreased A wave and B wave responses of the *Rho*^{P23H} retinas that tends to be exacerbated by IRE1α deficiency. (**B** and **D**) are photopic ERGs recordings at 2 and 3 months, respectively, that show no significant alteration with the exception of a small decrease in some of the B wave amplitudes (for **A** and **B**, n=10-18; for **C** and **D**, n=8-14). Similar distribution was observed between males and females. Data are presented as mean ± SEM. *p < 0.05, **p < 0.01 ***p < 0.001, ****p < 0.0001; two-way ANOVA.